Optimal Design and Operation of a Steel Plant Integrated with a Polygeneration System

Hamid Ghanbari
Thermal and Flow Engineering Laboratory, Chemical Engineering Department, Åbo Akademi University, Åbo 20500 Finland

Center for Advanced Process Decision-making, Chemical Engineering Department, Carnegie Mellon University, Pittsburgh, PA 15213

Henrik Saxén
Thermal and Flow Engineering Laboratory, Chemical Engineering Department, Åbo Akademi University, Åbo 20500 Finland

Ignacio E. Grossmann
Center for Advanced Process Decision-making, Chemical Engineering Department, Carnegie Mellon University, Pittsburgh, PA 15213

DOI 10.1002/aic.14098
Published online April 19, 2013 in Wiley Online Library (wileyonlinelibrary.com)

A process integration approach has been applied to integrate a traditional steelmaking plant with a polygeneration system to increase energy efficiency and suppress carbon dioxide emissions from the system. Using short-cut models and empirical equations for different units and available technologies for gas separation, methane gasification, and methanol synthesis, a mixed integer nonlinear model is applied to find the optimal design of the polygeneration plant and operational conditions of the system. Due to the complexity of the blast furnace (BF) operation, a surrogate model technique is chosen based on an existing BF model. The results show that from an economic perspective, the pressure swing adsorption process with gas-phase methanol unit is preferred. The results demonstrate that integration of conventional steelmaking with a polygeneration system could decrease the specific emissions by more than 20 percent. © 2013 American Institute of Chemical Engineers *AIChE J*, 59: 3659–3670, 2013
Keywords: process integration, polygeneration system, carbon dioxide emission, steelmaking, generalized disjunctive programming

Introduction

Traditional steelmaking is known as an energy intensive sector and a remarkable source of carbon dioxide emissions among primary industries. Improvement of the energy efficiency could increase the economic profitability and reduce environmental impact. In recent years, steel plants have experienced increasing expenses related to environmental issues, such as increase in carbon dioxide emission taxes. Parallel to this, the current financial crisis has made steelmakers face lower demand and falling prices, which have changed their business priorities to focus on lower operation costs, securing capital, and sustaining client relationship. These effects are more visible in steel companies in developed countries in comparison with major steel producers in the world, such as China and India.

Steelmaking processes are well-established and have already evolved to a mature state. It is, therefore, difficult to substantially reduce their energy demand and the emissions. A potential is still provided by an integration of steel plants with chemical plants, including carbon capturing and sequestration (CCS) and a polygeneration system. Due to tight integration of the power generation and the chemical synthesis sections, polygeneration systems have higher overall energy efficiency compared to stand-alone plants producing the same products.[1,2] Also the chemical products produced by a polygeneration plant can be used to substitute traditional liquid fuels, which is expected to results in cost-effective solutions for implementation of carbon dioxide capture and sequestration units.

Large amount of off-gases from the coke oven, blast furnace (BF), and basic oxygen furnace (BOF) are produced in traditional steelmaking. Today, these residual gases are used for heating (e.g., of steel slabs and preheating of combustion air) and in combined heat and power (CHP) plants. Zhang et al.[2] proposed a gas polygeneration strategy integrated with primary steelmaking to tackle the problem of energy efficiency and polluting emissions. The idea is to remove carbon

Additional Supporting Information may be found in the online version of this article.

Correspondence concerning this article should be addressed to H. Ghanbari at hghanbar@abo.fi.

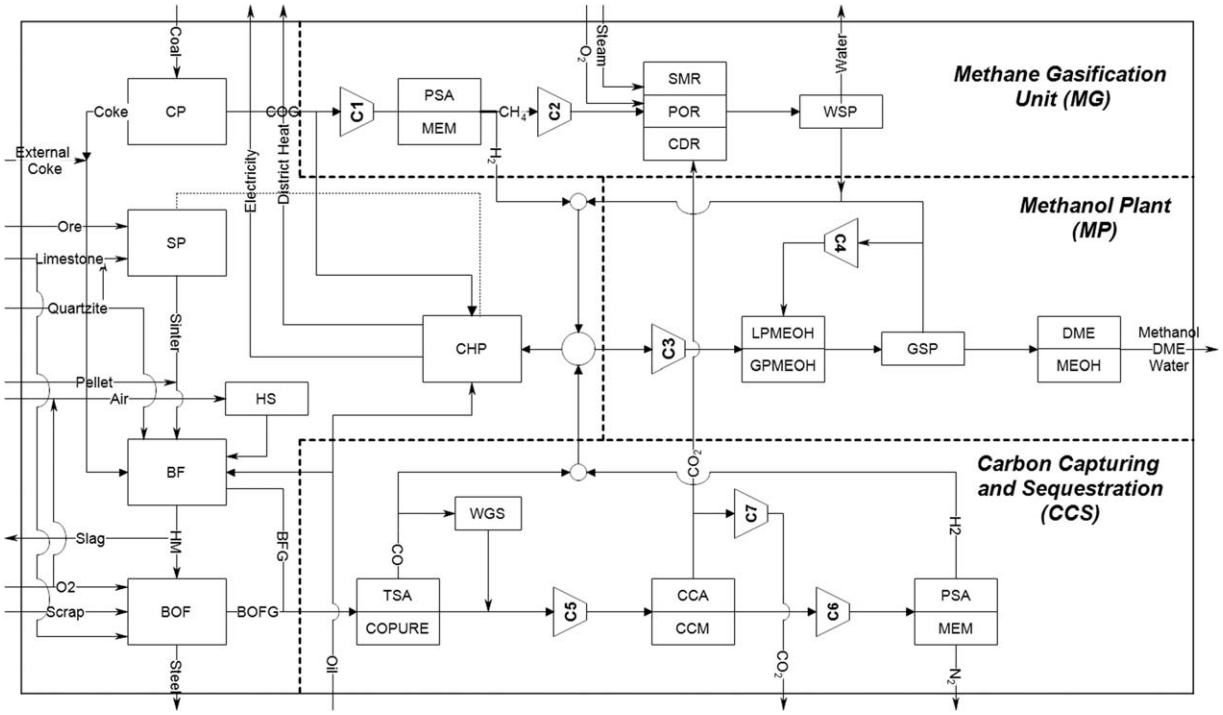

Figure 1. Integrated primary steelmaking with suggested polygeneration plant superstructure.

PSA: pressure swing adsorption, MEM: membrane adsorption, SMR: steam methane reforming, POR: partial oxidation reforming, CDR: carbon dioxide reforming, WSP: water separation, LPMEOH: liquid-phase methanol unit, GPMEOH: gas-phase methanol unit, GSP: gas separation unit, DME: dimethyl ether purification unit, MEOH: methanol purification unit, TSA: temperature swing adsorption, COPURE: chemical absorption unit, WGS: water gas shift unit, CCA: CO_2 chemical absorption, CCM: CO_2 capturing membrane, C1–C7: compressors, HM: hot metal, COG: coke oven gas, BFG: blast furnace gas, BOFG: basic oxygen furnace gas, CP: coke plant, SP: sinter plant, BF: blast furnace, BOF: basic oxygen furnace, HS: hot stoves, CHP: combined heat and power plant.

dioxide and use the residual gases as feedstock to a polygeneration system to produce district heat, electricity, and methanol as byproducts.

There have been several studies on optimal design of polygeneration systems. Liu et al.[1,3,4] studied a system with different feed-stocks and technologies that coproduces electricity and methanol. Their study showed that the conversion rate of technologies, the price of feedstock, the capital investment, and the fixed operating cost have strong influence on the net present value (NPV). They also presented a multiobjective mixed-integer nonlinear programming formulation of a typical polygeneration process operating over a time horizon where both profitability and environmental impacts were considered.

Chen et al.[5,6] proposed a coal and biomass-based polygeneration system to produce power, liquid fuels, and chemicals under different economic scenarios using nonlinear programming. They also performed a simultaneous optimization, analyzing the design and the operational decision variables. The results showed that higher NPVs can be obtained with increasing operational flexibility.

Ghanbari et al.[7,8] studied the possibilities to suppress carbon dioxide emissions and to increase the energy efficiency of an integrated steel plant under different scenarios of carbon dioxide emission and sequestration costs, different BF technologies and alternative fuels. Nonlinear programming was applied to tackle the optimization problem, particularly focusing on the performance of the BF operation as the core of the system. The potential of partially replacing coke with different fuels, such as oil, natural gas, and biomass simultaneously applying different technologies of BF operation (top gas recycling, cold oxygen injection, and massive hot blast oxygen enrichment) was investigated in a steel plant integrated with a polygeneration system. The results indicated a strong potential of combining process integration with the implementation of new BF technologies; it was found that the carbon dioxide emissions could be reduced by more than 50% in comparison with conventional steelmaking.

In the study of this article, a superstructure with common possible technologies for gas separation, methane gasification (MG), and methanol production (MP) has been proposed with the aim to investigate the optimal design and operation of the whole integrated steel and polygeneration system. Shortcut models and empirical equations based on a Finnish steel plant are used for some of the unit processes. Due to the complexity of the BF operation, a surrogate model based on partial least-square regression, and the Kriging method was developed to simulate the performance of the furnace in the system. The main difference between the suggested system of this study and a stand-alone polygeneration lies in the composition of the feedstock which is reliant on the operational state of the steel plant.

Process and Model Description

Figure 1 presents a conventional primary steelmaking plant integrated with a polygeneration system and a carbon capturing plant. It includes a coke plant (CP), sinter plant (SP), BF, BOF, hot stoves for blast preheating and units for CCS, MG, MP, and CHP generation. A superstructure with all possible network configurations for the MG, MP, and CCS units is presented in the next section. The system comprises primary steelmaking from sintermaking and cokemaking through the BF up to liquid steel, so the process units for casting and rolling are not included in this study. In all

figures to follow, the main streams and unit processes are shown. The aim of the study is to find a compromise between economic (investment and operation cost) and environmental (specific carbon dioxide emission) aspects of the system.

Coke plant

Coke is still the main source of thermal energy and reductant in the BF operation. The cokemaking process involves carbonization of coal at high temperatures in the absence of air, where a series of physical and chemical changes take place with the evolution of gases and vapors, finally creating a solid lumpy residual, coke. Cokemaking products are coke, coke oven gas (COG), tar, and residual fuel oil. The main part of the coke goes to the BF, while a smaller amount of coke breeze goes to the SP. For practical reasons, the capacity of the coke production in the present study was considered to be fixed at an upper limit (55 *t*/h), so any deficit/excess of coke (after the requirement of the SP and BF) will be bought/sold. The conversion of coal to metallurgical coke in the CP is simply modeled by linear relations between the feed rate of coal and the flow rates of produced coke and COG.[9] The dry composition of COG is assumed to be constant and it contains carbon monoxide, carbon dioxide, hydrogen, nitrogen, oxygen, and methane. Due to a high amount of hydrogen and methane in the gas, the stream is considered as feedstock to a gasification unit and to CHP units in the polygeneration system to produce electricity and district heat.

Sinter plant

The sintering process is a pretreatment step in the production of iron, where fine particles of iron ore are agglomerated by partial melting to yield a strong lumpy burden material suitable as a feed in the BF. Agglomeration of the fines is necessary to enable the passage of hot gases and prevent fluidization during the subsequent BF operation. Coke feed rate, iron ore feed rate, and limestone feed rate were considered as main inputs to the SP unit and sinter and recovered heat as main products.[9] In the steelmaking plant studied in this article, the sintermaking capacity was limited, so external iron bearing materials may be needed to reach the desired steel production rate. In such cases, pellets from an external producer are used in the system in the range of 0–600 kg/t_{hm} (i.e., kilogram per ton of hot metal).

Blast furnace

The BF as the heart of the steel plant acts as a large shaft-like countercurrent heat exchanger and chemical reactor, where the agglomerated iron bearing burden is charged with coke in alternate layers. The combustion of coke, which is maintained by the supply of preheated air (blast), provides CO to reduce iron oxides to iron and provides energy to heat and melt the iron and impurities. As the main product, liquid metal, often referred to as hot metal, is obtained, which can be further refined to steel in the BOF (see below). Due to the complexity of the BF, a first-principles model[9] was used to generate a surrogate model based on partial least-squares[10] and Kriging[11] techniques. A data set of 5000 feasible states was generated by the original model, and autoscale preprocessing with contiguous block cross validation was applied to build and evaluate the surrogate model, expressed as

$$Z_m^{\mathbf{BF}} = A_{1,m} + \sum_{n=1}^{5} A_{2,m,n} X_n^{\mathbf{BF}} \tag{1}$$

where $A_{1,m}$ and $A_{2,m,n}$ are regression coefficients, $X_n^{\mathbf{BF}}$ $(n = 1, \ldots 5)$ stands for hot metal production rate, specific oil rate, pellet rate, blast oxygen content, and blast temperature, which are the five inputs to the BF model. The 15 outputs $Z_m^{\mathbf{BF}}$ $(m = 1, \ldots, 15)$ in the surrogate model are the specific coke rate, volume flow rate of top gases, composition of top gases (H_2, N_2, CO_2, CO), top gas temperature, sinter flow rate, blast volume flow rate, (raceway) flame temperature, burden residence time, bosh gas volume, limestone feed flow rate, quartz feed flow rate, and slag flow rate[9] (Table 2). For the last three terms, the determination coefficients based on the partial least-squares algorithm was found insufficient. Hence, the Kriging algorithm was used based on polynomials of order zero and Gaussian correlation. The resulting surrogate model is expressed as

$$\hat{Z}_{\mathbf{m}}^{\mathbf{BF}} = \mu_m + \prod_s \gamma_{sj} \mathbf{exp}\left(-\theta_{mn} d_{ns}^2\right) \tag{2}$$

where μ_m is the generalized least-squares estimate for the polynomial term, θ_{mn} is the correlation function parameters, $d_{ns}^2 = \left(X_{\mathbf{n}}^{\mathbf{BF}} - w_{sn}\right)$ are the differences between a point and the design sites w_{sn}, and s is the number of random points (here, $s = 49$) that have been generated by the Latin hypercube method.[11]

Basic oxygen furnace

In the BOF, a mixture of hot metal, scrap, and limestone is charged into the refractory-lined steelmaking furnace and then oxygen is injected into the molten mixture at supersonic speed, resulting in oxidation of carbon and impurities, producing liquid crude steel (ls) with typically 0.1–0.5 wt % of carbon, and steelmaking slag. A general mass balance is used based on known hot metal flow, considering constant composition of top gases (mainly CO and CO_2) and that 50% of them can be recovered. For the sake of simplicity, the feed of scrap was assumed to be one fourth of the mass of hot metal in the feed.[9]

Carbon capturing and sequestration

An integration of a carbon dioxide capturing unit with a polygeneration system could be a long-term solution for suppressing CO_2 emissions from steel plants. BF top gas contains more than 20 vol % of carbon monoxide, which could be used to produce high-value chemical byproducts, such as methanol. It also contains more than 20 vol % carbon dioxide which could be captured and sequestrated; therefore, it is possible to suppress emissions from a conventional steel plant by exporting carbon from the system in the form of byproducts.[7,8] Figure 2 shows the unit processes for a CCS plant for gases from the BF and BOF. Three major units with two different CO, CO_2, and H_2 separation technologies are included in the study to find the optimal design for the CCS plant.

Recovery of carbon monoxide

To recover the carbon monoxide from gas streams, the most common methods used are liquefaction, chemical absorption, and selective adsorption. Liquefaction is not suitable in the present application due to relatively high nitrogen concentration in the BF top gas, because CO and N_2 are very similar in nature, which makes their separation by physical means difficult. For chemical absorption, the COPure^{SM} process[12] can be used to selectively separate carbon monoxide from the BF top gas. Low-pressure and temperature

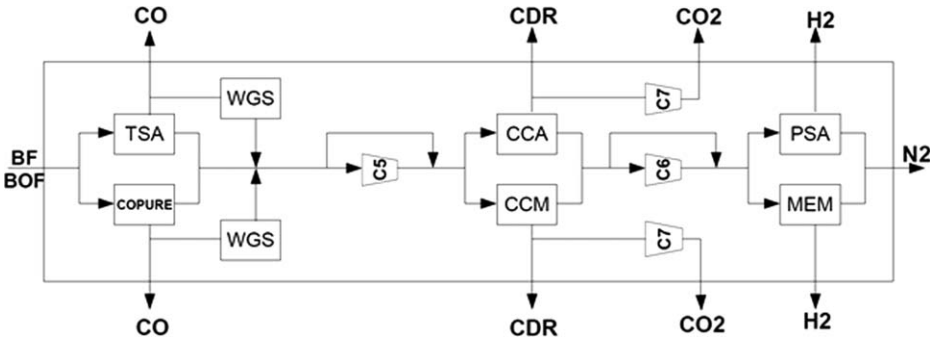

Figure 2. Carbon capturing and sequestration unit in the superstructure.

TSA: temperature swing adsorption, COPURE: chemical absorption unit, WGS: water gas shift reactor, CCA: CO_2 chemical absorption, CCM: CO_2 capturing membrane, CDR: carbon dioxide reforming, PSA: pressure swing adsorption, MEM: membrane separation.

operation and a noncorrosive solvent make the process strongly economical in terms of capital and operation costs. Reported carbon monoxide recovery and purity exceed 98 and 99%, respectively. The approximate utility requirements, for example, electrical power, reboiler and cooling duties, steam needed, and investment cost were estimated based on private communication with Rockey Costello, R.C. Costello & Associates.

Rabo et al.[13] suggested a temperature swing adsorption (TSA) process to selectively adsorb carbon monoxide from gas streams with an adsorbent mass comprising crystalline zeolite molecular sieves. Pressure is not a critical factor and temperature changes between 273 and 573 K are allowed, still yielding 99% recovery of carbon monoxide. This process can purify a gas stream containing as little as 10 ppm by volume of carbon monoxide, but it is preferred to use the process to make bulk separation of CO from gas streams containing at least 5 vol % carbon monoxide.

Recovery of carbon dioxide

Several studies have been presented on how to capture carbon dioxide from coal- or gas-fired power plant in the post combustion route.[14] Although it would seem reasonable to treat the top gas from BFs in the same way, there are some important differences, such as partial pressure of carbon dioxide and the lack of oxygen, which makes solvent degradation less likely. Tobiesen et al.[15] studied carbon dioxide chemical absorption with different amines, and Lie et al.[16] presented a membrane technology (CO_2 capturing membrane) for CO_2 recovery from BF top gas to attain a lower cost of capturing and storage for carbon dioxide. These two carbon capturing approaches are used in the superstructure of this study. For chemical absorption,[15] the process includes gas treatment, CO_2 removal, solvent regeneration, conditioning, and compression steps. The analysis showed that the lowest consumption of energy per ton carbon dioxide was achieved by combining 2-amino-2-methyle-1-propanol with intercooling. For the membrane process,[16] a fixed carrier site membrane with amine groups was suggested to selectively separate CO_2 from the BF top gas. In this process, the water in the feed gas is an advantage rather than a problem because the membrane should be humidified during the operation, which makes it a proper choice after sulfur scrubbing of the feedstock. The process takes place in two stages with low-temperature and pressure feedstock and carbon dioxide is sent to a pipeline at 110 bar.

Recovery of hydrogen

Pressure swing adsorption (PSA) and membrane separation are applied to find the optimal design to separate hydrogen from the residual gases of high nitrogen content. An efficient hydrogen recovery could be achieved by operating a PSA in a high pressure ratio of the feed over the residue or by a membrane in a high pressure ratio of the feed over the product, which may result in extra compression costs in both investment and operation.

The operational condition for a PSA process can be expressed as[17]

$$\frac{P_{\mathrm{PSA}}^{\mathrm{low}}}{P_{\mathrm{PSA}}^{\mathrm{high}}} = y_{H_2}^{F_{\mathrm{PSA}}}\left(1-\frac{R_{\mathrm{PSA}}}{1-\beta_{\mathrm{PSA}}}\right) \tag{3}$$

where $P_{\mathrm{PSA}}^{\mathrm{low}}$ and $P_{\mathrm{PSA}}^{\mathrm{high}}$ are the low and high absolute pressure of the pressure swing cycle, $y_{H_2}^{F_{PSA}}$ is the mole fraction of the hydrogen in the feed, R_{PSA} is the product recovery, and β_{PSA} is the adsorbent selectivity value, which relates to the flow rate and can be determined experimentally. In practice, the value of the hydrogen recovery is less than 0.92, and the adsorbent selectivity is greater than 0.02. The molar flow rates of the PSA process can be expressed as

$$f_{\mathrm{H_2}}^{\mathrm{p_{PSA}}} = R_{\mathrm{PSA}}\, f_{\mathrm{H_2}}^{F_{\mathrm{PSA}}} \tag{4}$$

$$f_{\mathrm{H_2}}^{\mathrm{bp\,PSA}} = f_{\mathrm{H_2}}^{F_{\mathrm{PSA}}} - f_{\mathrm{H_2}}^{\mathrm{p_{PSA}}} \tag{5}$$

$$f_{\mathrm{k}}^{\mathrm{bp\,PSA}} = f_{\mathrm{k}}^{F_{\mathrm{PSA}}} \tag{6}$$

where $f_{\mathrm{H_2}}^{\mathrm{p_{PSA}}}$: production stream, $f_{\mathrm{H_2}}^{\mathrm{F_{PSA}}}$: hydrogen in the feed stream, $f_{\mathrm{H_2}}^{\mathrm{bp\,PSA}}$: hydrogen in the byproduct stream, and $f_{\mathrm{k}}^{\mathrm{bp\,PSA}}$: other components in the byproduct stream.

For membrane technology, a Prism$^{\mathrm{TM}}$ separator[18] system developed by Air Product and Chemical is chosen. The unit is controlled by pressure and flow adjustment of gas streams. The separator uses the principle of selective permeation through a gas permeable membrane that has specially designed hollow fibers. Permeability coefficients of gases through a multicomponent membrane[19] are used to estimate the flow rate and operational pressure of the system. The operational pressure can be estimated by

$$\frac{P_{\mathrm{MEM}}^{\mathrm{low}}}{P_{\mathrm{MEM}}^{\mathrm{high}}} = \left(\frac{y_{H_2}^{F_{\mathrm{MEM}}}}{y_{\mathrm{H_2}}^{P_{\mathrm{MEM}}}}\right)\left(\frac{1-\zeta_{H_2}^{\mathrm{MEM}}}{1-y_{\mathrm{H_2}}^{F_{\mathrm{MEM}}}\zeta_{\mathrm{H_2}}^{\mathrm{MEM}}}\right) \tag{7}$$

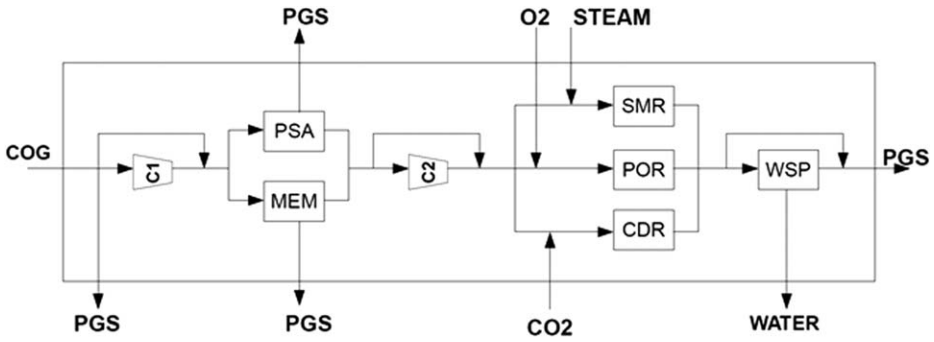

Figure 3. Methane gasification units in superstructure.

PSA: pressure swing adsorption, MEM: membrane adsorption, SMR: steam methane reforming, POR: partial oxidation reforming, CDR: carbon dioxide reforming, WSP: water separation unit, PGS: polygeneration system.

where $P_{\mathrm{MEM}}^{\mathrm{low}}$ and $P_{\mathrm{MEM}}^{\mathrm{high}}$ are the product and feed stream pressures, $y_{H_2}^{F_{\mathrm{MEM}}}$ and $y_{H_2}^{p_{\mathrm{MEM}}}$ are the mole fraction of hydrogen in feed and in the product streams, and $\zeta_{\mathrm{H_2}}^{\mathrm{MEM}}$ is membrane hydrogen product recovery. The molar flow rate of the (hydrogen enriched) product stream and byproduct stream can be determined by

$$f_{H_2}^{p_{\mathrm{MEM}}} = \zeta_{\mathrm{H_2}}^{MEM} f_{\mathrm{H_2}}^{\mathrm{F_{MEM}}} \tag{8}$$

$$f_k^{\mathrm{p_{MEM}}} = \frac{\alpha_{\{k/H_2\}}\zeta_{\mathrm{H_2}}^{\mathrm{MEM}}\; y_{\mathrm{k}}^{F_{\mathrm{MEM}}} f_{\mathrm{H_2}}^{F_{MEM}}}{y_{\mathrm{H_2}}^{F_{\mathrm{MEM}}}\left[2-\zeta_{\mathrm{H_2}}^{\mathrm{MEM}}-\frac{\alpha_{(k/H_2)}\zeta_{H_2}^{\mathrm{MEM}}}{1-y_{H_2}^{F_{MEM}}\zeta_{H_2}^{\mathrm{MEM}}}\right]-2\left[\frac{y_{H_2}^{\mathrm{pMEM}}P_{\mathrm{MEM}}^{\mathrm{low}}}{P_{\mathrm{MEM}}^{\mathrm{high}}}\right]\left(1-\alpha_{\{k/\mathrm{H_2}\}}\right)} \tag{9}$$

$$f_{\mathrm{H_2}}^{b\mathrm{p_{MEM}}} = \left(1-\zeta_{\mathrm{H_2}}^{\mathrm{MEM}}\right) f_{\mathrm{H_2}}^{F_{\mathrm{MEM}}} \tag{10}$$

$$f_{\mathrm{k}}^{b\mathrm{p_{MEM}}} = f_{\mathrm{k}}^{F_{\mathrm{MEM}}} - f_{\mathrm{k}}^{p_{\mathrm{MEM}}} \tag{11}$$

where $\alpha_{\{k/H_2\}}$ is the ratio of the permeability coefficient of other components in the stream to hydrogen and the molar flow rates are $f_{\mathrm{H_2}}^{\mathrm{p_{MEM}}}$: hydrogen in the product stream, $f_k^{\mathrm{p_{MEM}}}$: other components available in the product stream, $f_{\mathrm{H_2}}^{b\mathrm{p_{MEM}}}$: hydrogen in the byproduct, and $f_{\mathrm{k}}^{b\mathrm{p_{MEM}}}$: other components in the byproduct stream.

Gas reforming plant

The COG is assumed to have a constant composition and it contains high amounts of hydrogen and methane which can be used directly in the polygeneration system or as feedstock to the gas-reforming plant. Figure 3 shows the alternative unit processes for the gasification route. PSA and membrane technologies are used to separate mainly hydrogen from methane, and steam methane reforming (SMR), carbon dioxide reforming (CDR), and partial oxidation reforming (POR) technologies are applied for MG to produce more hydrogen. The operational conditions of the separation processes are estimated by Eqs. 3–11. The main differences are in feedstock mass flow rates and compositions. In the gas reforming units, the optimal values of the critical parameters (temperature, pressure, and reactant ratio) have been taken from the literature based on standalone processes.

Production of synthesis gas from methane can be realized through SMR (13). This process is highly endothermic, but has low carbon deposition and high H_2/CO ratio which makes it suitable for methanol synthesis. The steam-methane reaction takes place with the water gas shift reaction (14)

$$\mathbf{CH_4 + H_2O = CO + 3H_2} \tag{12}$$

$$\mathbf{CO + H_2O = CO_2 + H_2} \tag{13}$$

The feedstock to the SMR unit is mixed with saturated steam in a methane-to-steam ratio of 3.68 kmol H_2O/kmol CH_4, and the reaction takes place at 20 bar and 1153−1300 K. The conversion of CH_4 and CO is considered to be $x_{\mathrm{CH_4}}^{\mathrm{SMR}} = 81.5$ % and $x_{\mathrm{CO}}^{\mathrm{SMR}} = 40.2$ %.[20] The heat of reaction at typical reformer operating conditions for the steam-methane reaction and water-gas shift reaction are 234.7 kJ/mol and −34.6 kJ/mol, respectively.

CDR of methane can be expressed as

$$\mathbf{CO_2 + CH_4 = 2\ CO + 2\ H_2} \tag{14}$$

and has a great potential to be used in chemical industry to gain more environmental benefits by suppressing carbon dioxide emissions. Wang et al.[21] showed that the optimal operating condition would be 1143−1313 K at a pressure of 1 bar, equal ratio of methane to carbon dioxide, and the conversion of methane in the reaction is $x_{\mathrm{CH_4}}^{\mathrm{CDR}} = 0.90$. The heat of reaction has been reported to be 247 kJ/mol at 298 K.

The third alternative technology for synthesis gas formation is the exothermic methane partial oxidation reaction with standard heat of reaction of −35.9 kJ/mol and is expressed as

$$\mathbf{CH_4 + 0.5\ O_2 = CO + 2\ H_2} \tag{15}$$

This process shows a high yield of hydrogen, but the oxygen stream makes it costly. Zhu et al.[22] showed that by increasing temperature, the selectivity of carbon monoxide and hydrogen increases, but pressure has a negative effect on methane conversion and hydrogen production. The investigators also showed that a ratio of $\frac{\mathrm{CH_4}}{\mathrm{O_2}} = 2$ and a temperature of 1073−1473 K at 1 bar are ideal conditions for an oxy-reforming reaction to get a high yield of the synthesis gas. The conversion of methane is considered to be $x_{\mathrm{CH_4}}^{\mathrm{POR}} = 0.95$.

The molar flow rates for the gas reforming units are calculated by (linear) mass balances for fixed conversion reactor with number of parallel reactions (NR) for each component k, and can be expressed as[23]

$$f_p^k = f_F^k + \sum\nolimits_{r=1}^{\mathrm{NR}} \gamma_r^k x_r f_F^{l(r)} \tag{16}$$

where r is the number of reaction, $l(r)$ is the limiting component, γ_r^k is the stoichiometric coefficient (which is

positive, negative, and zero for product, reactant, and inert components) and x_r is the fraction converted per pass based on limiting reactant.

The produced syngas passes through heat exchangers to cool down and, depending on the gasification units, is sent to a water removal column. The operational conditions considered are the blow dew point of water and complete condensation of water is assumed to occur. It is assumed that a small amount of carbon particles produced in the syngas generator due to coking are removed with the water, and the dry syngas is sent to the polygeneration plant.

Polygeneration plant

All the syngas from CCS and gasification units is distributed and used in the polygeneration system to produce methanol, electricity, and district heat. Methanol can be produced via two different technologies (Figure 4): gas-phase (GP) or liquid-phase (LP). In the GP MP, methanol is synthesized in a GP reaction over a heterogeneous catalyst from a synthesis gas that consists primarily of hydrogen, carbon monoxide, and carbon dioxide. Newer processes focus on the use of CO-rich synthesis gas instead of H_2-rich synthesis gas, thereby using cheaper synthesis gas for the production of methanol. One of the promising technologies using CO-rich synthesis gas is the LP methanol synthesis process. The single-pass conversion of syngas in the LP reactor is, however, still limited.[24]

Three main reactions take place in the synthesis of methanol

$$\mathbf{CO} + 2\ \mathbf{H_2} = \mathbf{CH_3OH} \tag{17}$$

$$\mathbf{CO_2} + 3\ \mathbf{H_2} = \mathbf{CH_3OH} + \mathbf{H_2O} \tag{18}$$

$$2\mathbf{CO} + 4\mathbf{H_2} = \mathbf{C_2H_6O} + \mathbf{H_2O} \tag{19}$$

The heats of reaction for the first and the second reaction at standard temperature and pressure are -90.8 kJ/mol and -49.5 kJ/mol, respectively. Also the third reaction (Eq. 19) takes place as a side reaction in the GP, producing dimethyl ether (DME) to a limited extent with a reaction heat of -204.9 kJ/mol at standard conditions.

In the GP reactor, carbon monoxide, carbon dioxide, and hydrogen are catalytically converted to methanol and DME. Typical operating conditions are 50 bar and 533 K, and all reactions are exothermic and the excess heat must be removed to maintain optimum operational conditions. The conversion is dependent on temperature, pressure, hydrogen to carbon monoxide ratio, gas hourly space velocity, catalyst composition, and carbon dioxide content. The overall conversion of the carbon monoxide and carbon dioxide in the syngas to methanol is typically 0.95 and methane and nitrogen are considered as inert. The amount of DME produced is 2 wt % of the methanol produced.[20,24] The product stream is cooled down to 318 K to condense all methanol, DME, and water. Unreacted H_2, CO, CO_2, CH_4, and N_2 do not condense at the conditions of the exchanger and must be recovered in a flash drum and sent to utility to be burned. DME can be separated from methanol by extractive distillation at 11.2 bar and a reflux ratio of 20 mol recycled liquid/mol distillate. In this column, almost complete recovery of dimethyl can be assumed, which is accomplished as a top product while methanol and water leave at the bottom. DME can be used as an additive to diesel.

Even though the operation conditions are similar to the GP process, the LP methanol process has some advantages, such as ability to control temperature, achieving higher conversion per pass with the same H_2/CO ratio (≥ 2), the heat of reaction can be more effectively used to generate high-pressure steam, and catalyst can be added and withdrawn from the system while on stream without the necessity to shutting down the process. However, the conversion per pass in the LP reactor in CO-rich syngas is low and, therefore, the methanol yield is also low. LP methanol operational conditions depend on reactor pressure, temperature, composition of the feed syngas, which per pass conversion of syngas to methanol may vary from 15% to as high as 60%. Equations 17 and 18 are considered as the main reactions, and the reactor typically operates at 523 K and 50 bar. The conversion of carbon dioxide in Eq. 18 is assumed to be fixed at 8.9% and carbon monoxide conversion is estimated to be 30.6%.[24]

The product stream is sent to heat exchanger to condense methanol and water from the unreacted gases. In the methanol separator, a simple-phase separation takes place and the bottom product is sent to the methanol distillation column, and the unreacted syngas is recovered to recycle or sent to the power generation plant.

At the final stage, in the methanol, distillation column water and methanol are separated at 3.4 bar and 318 K with 99.9% of methanol purity as top product at a reflux ratio of 1.5. Water with remaining methanol leaves as the bottom product of the distillation column and is sent to a waste water treatment facility.

Combined heat and power units

In the CHP plant, the syngas is modeled to be burned to release heat at high temperature to produce high-pressure steam for a turbine, with given efficiency factors in the turbine and in the generator. The low-pressure steam is finally condensed, releasing heat for district heat production. To estimate the electricity and district heat that could be sold, energy balances for the main processes such as compressor, reactors, and purification columns are used to calculate the internal power requirement. The energy used in the compressor is first calculated for the isentropic reference case, and the true operation is estimated with adiabatic, motor drive, and mechanical efficiencies of $\eta_{ad} = 0.9$, $\eta_{md} = 0.9$ and $\eta_{mech} = 0.85$, respectively. The outlet temperature, standard enthalpy and compressor work (W_{comp}) are calculated by

$$\frac{T_{\mathbf{out}}}{T_{\mathbf{in}}} = \left(\frac{P_{\mathbf{out}}}{P_{\mathbf{in}}}\right)^{(\bar{\gamma}-1)/\bar{\gamma}} \tag{20}$$

$$H_k - H_{k,298} = B_{1k}\ T + B_{2k}\left(\frac{T^2}{2}\right) + B_{3k}\left(\frac{T^3}{3}\right) + B_{4k}\left(\frac{T^4}{4}\right) - \left(\frac{B_{5k}}{T}\right) + B_{6k} - B_{7k} \tag{21}$$

$$W_{comp} = \frac{\sum_k f_k\ (H_{out,k} - H_{in,k})}{\eta_{ad}\ \eta_{md}\ \eta_{mech}} \tag{22}$$

where T_{out} and T_{in} are the outlet and inlet absolute temperatures, P_{out} and P_{in} are the outlet and inlet pressures, $\bar{\gamma}$ is

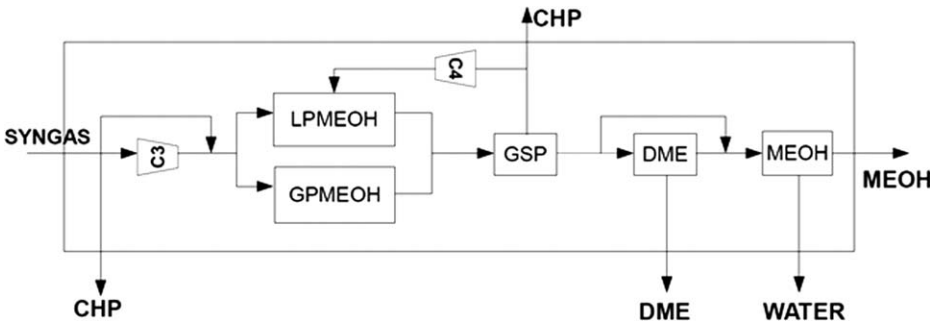

Figure 4. Methanol production units in superstructure.

CHP: combined heat and power plant, LPMEOH: liquid-phase methanol reactor, GPMEOH: gas-phase methanol rector, GSP: gas separation unit, DME: dimethyl ether purification, MEOH: methanol purification.

the average specific heat ratio of the components in question, T is the absolute temperature, H_k is the standard enthalpy in kJ/mol, and B_k are the parameters obtained from NIST Chemistry WebBook.[25]

In the energy balance equation for the reactors based on inlet and outlet composition, temperature, and pressure, the enthalpy change within the reactor is calculated by Eq. 21. The outlet temperature and pressure is considered to be the same as reactor operational condition. The heat of reaction at standard condition is added to calculate the enthalpy change in each specific reactor.

In the process, several heat exchangers are used to elevate the streams to the operational temperature in the unit. The enthalpy change through an exchanger is calculated based on the change of enthalpy from inlet to outlet temperature, and the thermal efficiency is assumed to be 0.7. To estimate the energy required in the distillation columns, the enthalpy supplied in reboiler, $\Delta H_{\text{reb.}}$ is calculated by

$$\Delta H_{\text{reb.}} = \Delta H_{\text{cond.}} + \Delta H_{\text{sensible}} \tag{23}$$

$$\Delta H_{\text{cond.}} = \sum_k (\bar{R}+1)\, f_k\, H_k^V \tag{24}$$

$$\Delta H_{\text{sensible}} = \sum_k f_k\, C_{P_k}\, \Delta T_{\text{sensible}} \tag{25}$$

where $\Delta H_{\text{cond.}}$ is the enthalpy change to condense the distillate product (kJ/mol), $\bar{R}$ is the reflux ratio, H_k^V is the heat of vaporization at given temperature (kJ/mol), $\bar{C}_{P_k}$ is the specific heat capacity of the distillate component (kJ/(mol · K)), $\Delta T_{\text{sensible}}$ is difference of boiling point of distillate product and feed temperature (K), and subscript k denotes components in the distillate stream.

In the total energy balance of the system, all heat needed in different units, work done by compressors, and heat removed by heat exchangers are summed. Also the excess syngas and external oil, if necessary, are considered as fuel in the power plant.

Objective function

To find the optimal design and operation of the suggested superstructure, considering 40% tax rate, 12% annual discount rate, 10 and 30 years life and depreciation time of the project, and 7500 h annual operating time,[5] the NPV was chosen as the objective function

$$\text{NPV} = -0.893\ CI + 5.65\text{NP} \tag{26}$$

where CI is the total capital investment cost of equipment for gasification, CCS, and methanol units, which are expressed by a linear approximation with fixed cost charge of the Guthrie's modular method with cost update factor for 2010.[23] NP is the annual net profit of the integrated system, which is estimated from the product's profit reduced by the sum of operating, carbon emission tax, and carbon sequestration costs. Table 1 shows the purchasing and selling price for feedstock and products of the system used in the study. The carbon emissions from the system are calculated based on a carbon balance equation, including all carbon-bearing inputs (coal, oil, external coke, limestone) and excluding the outflows of carbon in liquid steel, methanol, and sequestrated carbon dioxide.

Optimization problem

A generalized disjunctive programming approach is applied to model the proposed superstructure of an integrated steel plant with a polygeneration system. After selecting an alternative, the corresponding need for compressors and the heat exchangers will be imposed. If a process unit is chosen, then the mass and energy balances are enforced and the corresponding cost term is considered.

Table 1. Costs in Objective Function

C_{ore}	104 \$/t
C_{pellets}	156 \$/t
C_{coal}	143 \$/t
$C_{\text{coke,ext}}$	390 \$/t
C_{oil}	195 \$/t
$C_{\text{limestone}}$	39 \$/t
C_{quartz}	39 \$/t
C_{O_2}	65 \$/km^{3}n
C_{scrap}	130 \$/t
C_{methanol}	325 \$/t
$C_{\text{dimethyle ether}}$	200 \$/t
$C_{\text{liquid steel}}$	550 \$/t
$C_{\text{electricity}}$	65 \$/MW
$C_{\text{district heat}}$	13 \$/MW
C_{emission}	0−150 \$/t
$C_{\text{sequestration}}$	0−150 \$/t

$$\textbf{Max} \quad \textbf{NPV}$$

$$hm(f_j, x_j) = 0 \qquad j \in \{\text{BF}\}$$
$$A^j f_j = b^j \qquad j \in \{\text{WSP, GSP, C1, C7, MEOH, CHP, CP, SP, HS, BOF}\}$$
$$hc(f_j) = 0 \qquad j \in \{\text{WSP, GSP, C1, C7, MEOH}\}$$
$$he(f_j, H_j) = 0$$

$$\begin{bmatrix} Y_{\text{PSA}} \\ hm(f_{\text{PSA}}, R_{\text{PSA}}) = 0 \\ hp(f_{\text{PSA}}, x_{\text{PSA}}, R_{\text{PSA}}, \beta_{\text{PSA}}) = 0 \\ he(f_{\text{PSA}}, T_{\text{PSA}}) = 0 \\ hc(f_{\text{PSA}}) = 0 \end{bmatrix} \vee \begin{bmatrix} Y_{\text{MEM}} \\ A^{\text{MEM}} f_{\text{MEM}} = b^{\text{MEM}} \\ hp(f_{\text{MEM}}, x_{\text{MEM}}) = 0 \\ he(f_{\text{MEM}}, T_{\text{MEM}}) = 0 \\ hc(f_{\text{MEM}}) = 0 \end{bmatrix}$$

$$\vee_{\text{reac}} \begin{bmatrix} Y_{\text{reac.}} \\ A^{\text{reac}} f_{\text{reac.}} = b^{\text{reac}} \\ he(f_{\text{reac}}, T_{\text{reac}}) = 0 \\ hc(f_{\text{reac}}) = 0 \end{bmatrix} \qquad \forall \text{reac.} \in \{\text{SMR, CDR, POR}\};\ \forall \text{reac.} \in \{\text{LPMEOH, GPMEOH}\}$$

$$\vee_{\text{sep}} \begin{bmatrix} Y_{\text{sep}} \\ A^{\text{sep}} f_{\text{sep}} = b^{\text{sep}} \\ he(f_{\text{sep}}, T_{\text{sep}}) = 0 \\ hc(f_{\text{sep}}) = 0 \end{bmatrix} \qquad \forall \text{sep} \in \{\text{TSA, COPURE}\};\ \forall sep \in \{\text{CCA, CCM}\}$$

$$\begin{bmatrix} Y_{\text{DME}} \\ A^{\text{DME}} f_{\text{DME}} = b^{\text{DME}} \\ he(f_{\text{DME}}, T_{\text{DME}}) = 0 \\ hc(f_{\text{DME}}) = 0 \end{bmatrix} \vee \begin{bmatrix} \neg Y_{\text{DME}} \\ f_{\text{DME}} = 0 \\ he = 0 \\ hc = 0 \end{bmatrix}$$

$$\vee_{\text{comp}} \begin{bmatrix} Y_{\text{comp.}} \\ A^{\text{comp}} f_{\text{comp.}} = b^{\text{comp}} \\ hp(P_{\text{comp}}, T_{\text{comp}}) = 0 \\ he(f_{\text{comp}}, T_{\text{comp}}, P_{\text{comp}}) = 0 \\ hc(f_{\text{comp.}}) = 0 \end{bmatrix} \qquad \forall \text{comp} \in \{C2 : C6\}$$

$$Y_{sep} \Rightarrow \left(P_{sep} \geq P^{min}, T_{sep} \geq T^{min}\right) \qquad \forall \text{sep}$$
$$Y_{\text{reac}} \Rightarrow \left(P_{\text{reac}} \geq P^{\text{min}}, T_{\text{reac}} \geq T^{\text{min}}\right) \qquad \forall \text{reac}$$
$$\neg Y_{\text{sep}} \Rightarrow Y_{\text{comp}} \qquad \forall \text{sep, comp}$$
$$\neg Y_{\text{reac}} \Rightarrow Y_{\text{comp}} \qquad \forall \text{reac, comp}$$
$$Y_{\text{GPMEOH}} \Rightarrow Y_{\text{DME}}$$
$$Y_{\text{sep}}, Y_{\text{comp}}, Y_{\text{reac}}, Y_{\text{DME}}, Y_{\text{PSA}}, Y_{\text{MEM}} \in \{\text{True, False}\} \qquad \forall \text{ sep, comp, reac, PSA, MEM, DME}$$
$$f^L \leq f \leq f^U$$
$$x^L \leq x \leq x^U$$

where *sep* refers to the separation units, *comp* to the compressors, *reac* to the reactor units, and Y is a Boolean variable. The mathematical model and notations are described in Supporting Information. The big-M formulation[23] is used to transfer the generalized disjunctive programming model to a mixed integer nonlinear programming (MINLP) model in GAMS[26] and is solved to global optimality. The model has 20 binary variables, 1069 continuous variables, and 1924 constraints. The problem is nonconvex mainly due to bilinear terms in mass balances and in enthalpy estimation equations. Table 2 shows upper and lower bounds on some variables imposed by the operational condition in the steelmaking process.

Results

Optimal design

Figure 5 shows the optimal solution for the suggested superstructure found by using BARON[27] as the global optimization solver and DICOPT[28] as alternative MINLP solver in GAMS for a steel production rate of 150−170 t_{ls}/h and carbon dioxide emission and sequestration cost of 52 and 26 \$ per ton CO_2. Both solvers find the optimal production rate to be at maximum steel production with a NPV of 2.0453 G\$. To solve a single-optimization problem, BARON (with a relative gap of 10^{-4}) required more than 37 h, whereas DICOPT needed only slightly more than 2 s of computation time (on a dual core 2.67-GHz CPU). Due to a large number of scenarios to be investigated, DICOPT was chosen as the method to find the optimum of the conceptual design for the superstructure at different emission and sequestration costs and production rates, despite the risk of not finding the global optimum.

Analysis of the results show that the feedstock to the gasification unit from COG is compressed to 28 bar and passed

Table 2. Upper and Lower Bounds for Some Variables

Variable	Range
Steel production rate	150−170 t_{st}/h
BF blast oxygen content	21−32 vol %
BF specific oil rate	0−120 kg $/t_{hm}$
BF blast temperature	250−1200 C
BF specific pellet rate	0−600 kg $/t_{hm}$
BF flame temperature	1800−2300 C
BF top gas temperature	115−250 C
BF bosh gas volume	150−220 km^3n/h
BF solid residence time	6.0 − 9.5 h
BF slag basicity	1.0−1.2
BF sinter feed flow	0−160 t/h
BF own coke feed flow	0−55 t/h
Pressure	1−150 bar
Adsorbent selectivity	0.02−2
Hydrogen recovery	0.8−0.92

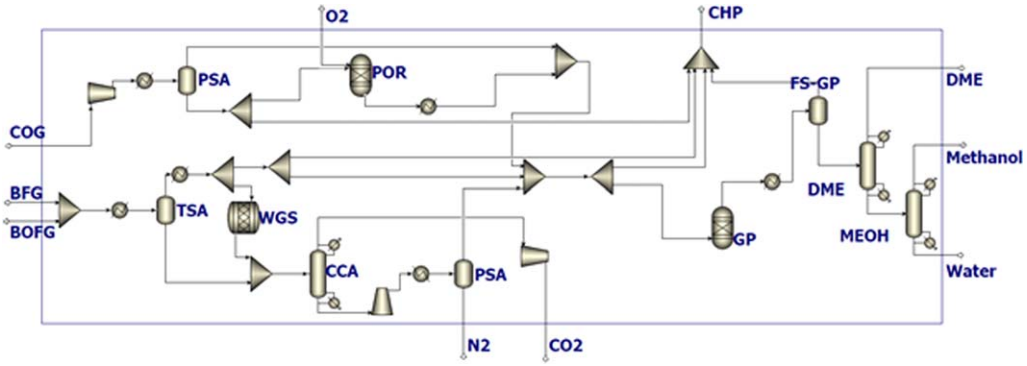

Figure 5. Optimal process designs for the polygeneration system.

PSA: pressure swing adsorption, POR: partial oxidation reactor, GP: gas-phase methanol rector, FS-GP: gas separation unit, DME: dimethyl ether purification, MEOH: methanol purification, TSA: temperature swing adsorption, WGS: water gas shift reactor, CCA: CO_2 chemical absorption. [Color figure can be viewed in the online issue, which is available at wileyonlinelibrary.com]

through a heat exchanger to reach the operational condition of the feed stream of the PSA for hydrogen separation. The hydrogen recovery and adsorbent selectivity values take on their upper and lower boundary values (0.92 and 0.02), respectively. The top product stream is sent to the methanol plant and the bottom stream, which is methane enriched, is partly sent to power plant and to the partial oxidation reactor. The cooled product of reaction is sent to the methanol plant. The mixture of BF and BOF gases passes through a heat exchanger to attain the required temperature for carbon monoxide recovery in the TSA step. The product stream is considered to distribute between the water gas shift reactor to produce more hydrogen and the polygeneration plant.

The bottom byproducts of TSA and water gas shift are sent to the CO_2 capturing unit. The removed carbon dioxide is compressed to 100 bar for sequestration. The byproduct of the chemical absorption unit contains mainly nitrogen and hydrogen. This stream is also compressed to 110 bar and sent to PSA to separate hydrogen and nitrogen. The hydrogen recovery and adsorbent selectivity parameter are estimated to be 0.90 and 0.02, respectively. The recovered hydrogen is sent to the methanol unit and the bottom product, which is mostly nitrogen, is purged to the atmosphere. The products of the methanol reactor are cooled to 318 K, where methanol, DME, and water are condensed and purified, and the residual gases are sent to the power plant. Table 3 shows some of the optimal variables for the system (left column) and the results of a sequential NLP optimization of an integrated steelmaking with complex BF model and steam reforming plant.[8]

The results show that in the optimal operation condition of the integrated system, the BF works at lower coke rate and lower blast temperature which leads to no extra fuels in power plant. On the other hand, with lower exporting carbon as byproduct (methanol) from the system, both the specific emission of carbon dioxide per liquid steel and steel cost decrease.

Table 3. Optimal Process Variables for the System with a Steel Production Rate of 170 t_{ls}/h, Costs of Emissions c_e= 52 \$/t_{CO2}, and Sequestration c_{seq}= 26 \$/t_{CO2}

Variable	[a]	[b]
Blast volume (km^3n/h)	123.6	126.8
Blast oxygen (vol %)	27.8	28.0
BFG volume (km^3n/h)	199.1	203.0
Sinter feed rate (t/h)	**160.0**	**160.0**
Specific coke rate (kg/t_{hm})	309.4	320.7
Specific oil rate (kg/t_{hm})	120.0	**120.0**
Specific pellet rate (kg/t_{hm})	459.4	457.6
Flame temperature (°C)	**2300**	2246
Blast temperature (°C)	990	**1200**
Bosh gas volume (km^3n/h)	181.0	186.0
Top gas temperature (°C)	128.0	143.0
Burden residence time (h)	7.4	7.3
Slag rate (kg/t_{hm})	216.0	216.4
COG volume (km^3n/h)	17.6	17.6
BOFG volume (km^3n/h)	6.2	6.5
Aux. fuel excluding BF (t/h)	0.0	9.3
Bought/sold coke (t/h)	0.0	0.0
Sold methanol (t/h)	18.8	28.6
Specific emission (t_{CO2}/t_{ls})	0.97	1.50
Specific steel cost (\$/t_{ls})	311.2	334.6

The left column is the results for present study and the right column data are from earlier work by the authors.[8] Boldface denotes a value at its constraint.
[a]Integrated steelmaking with blast furnace surrogate model, auxiliary oil injection, and POR/MEOH Plant (MINLP model).
[b]Integrated steelmaking with complex blast furnace model, auxiliary oil injection, and SMR/MEOH plant (NLP model[8]).

Optimal conditions at constant steel production rate

The optimal design of an integrated steel plant with a polygeneration system coproducing methanol, electricity, and district heat is next investigated in different scenarios of carbon dioxide sequestration and emission costs. Even though the penalty for carbon emissions in the European union (EU)

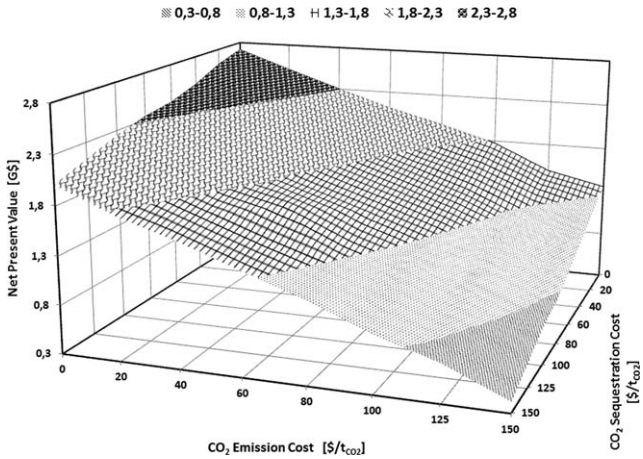

Figure 6. Net present value at different specific emission and sequestration costs for a hot metal production rate of 150 t_{hm}/h.

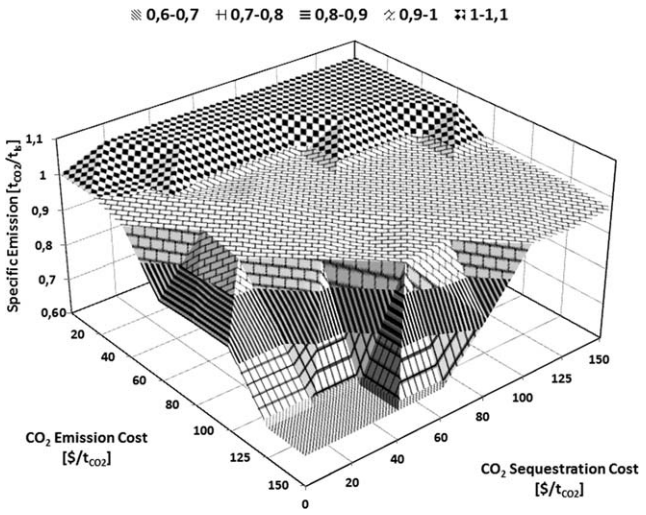

Figure 7. Optimal specific emission at different carbon dioxide emission and sequestration costs for a hot metal production rate of 150 t_{hm}/h.

has varied on a low level (5–20 €/t_{CO2}), it has been estimated that a tax level of 50–100 €/t_{CO2} in the future would be necessary for making a sufficient impact on industrial production. Likewise, the estimated costs of CO_2 storage, including liquefaction and transport, vary considerably depending on the location and deposition technology. Therefore, the two costs were varied within a large range (0–150 \$/ t_{CO2}) in this study.

Figure 6 shows the NPV of the system as a function of carbon dioxide emission and sequestration costs. The results estimate a 2.5 G\$ change between the lowest and the highest cost scenarios. They show that the effect of the emission cost on the NPV is stronger at high sequestration cost, and that it is higher than the effect of the sequestration cost.

Figure 7 depicts the specific emissions (i.e., ton carbon dioxide per ton liquid steel) from the system at constant hot metal production rate (150 t_{hm}/h) and carbon dioxide emission and sequestration costs of 0–150 \$/t_{CO2}. In different scenarios, the specific carbon dioxide emission changes from 0.68 t_{CO2}/t_{ls} to 1.05 t_{CO2}/t_{ls}, which is clearly lower than for a corresponding conventional steel plant (1.6–1.7 t_{CO2}/t_{ls}). Quite naturally, the lowest specific emission is obtained for a high emission price and low sequestration cost. The analysis shows that at higher sequestration cost the model prefers the CDR process and, therefore, part of the carbon dioxide has been sent to the MG unit. For high carbon dioxide emission cost and low sequestration cost, a higher amount of carbon dioxide is sent for sequestration and the LP methanol reactor has been the choice. The MP for the different scenarios is estimated to be between 18 and 23 *t*/h. Finally, it is interesting to note that the specific emissions exhibit a plateau (i.e., are constant) for the optimal states in the cases where the cost of emission roughly equals the cost of sequestration.

Sensitivity analysis of main raw materials and products

A simple sensitivity analysis was undertaken to estimate the effect of changing the main feedstock material and product prices at a constant steel production rate (170 t_{ls}/h) and costs of emission and sequestration of 52 \$/t_{CO2} and 26 \$/t_{CO2}. The variation of the NPV of the system by a change of ±50% in the price of the main four input materials (oil, coal, ore, and pellets) and four products (methanol, steel, electricity, and district heat) is depicted in **Figure** 8. As expected, it illustrates that the NPV increases by increasing the price of products and decreases by increasing the prices of the feed materials. The oil rate does not have the same effect on NPV because by decreasing the price of oil the MP increases and more oil has to be used in the power plant. In the considered scenario of emission and sequestration costs, changing the price of electricity and district heat does not have any effect on NPV as no external electricity and district heat are produced in the optimal states. Obviously, the steel price is of primary importance among the products and raw materials: for a 50% increase in the price of steel, the NPV of the system increases by +138%, while no feasible solution was found if the price of liquid steel decreases by 50%.

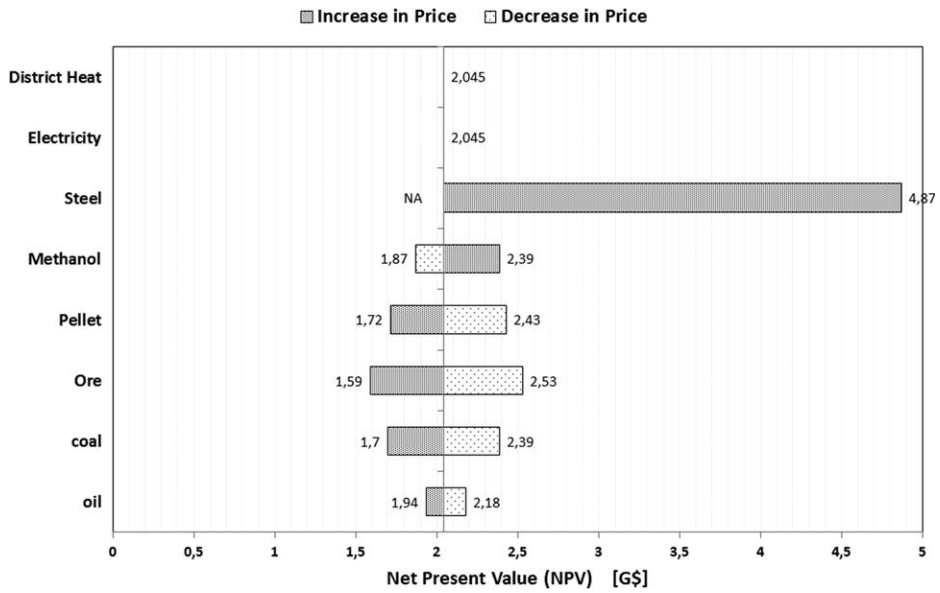

Figure 8. Optimal net present value for a ±50% change in main raw material and product costs at a constant production rate of 170 tls/h and cost of emission and sequestration of 52 \$/tCO2 and 26 \$/tCO2.

Table 4. Specific Emissions, Liquid Steel costs, Net Present Value, and Methanol Production Rate for Different Hot Metal Production Rates

Production Rate (t_{hm}/h)	Specific CO_2 Emission (t_{CO2}/t_{ls})	Liquid Steel Cost ($/$t_{ls}$)	Net Present Value (G$)	Methanol Production (t/h)
130	1.02	307.6	1.82	15.1
135	1.01	308.4	1.88	15.7
140	0.99	309.6	1.95	16.5
145	0.99	311.0	2.00	17.3
150	0.98	311.3	2.06	19.5

Costs of emission and sequestration are constant (52 $/tCO2 and 26 $/tCO2).

Optimal conditions for variable hot metal production rate

Table 4 reports the optimal liquid steel production cost, NPV and specific carbon dioxide emission, and MP rate for different hot metal production rates at constant carbon dioxide emission, and sequestration costs of 52 and 26 $/$t_{CO2}$. The results illustrate that by increasing the production rate, liquid steel cost increases and specific CO_2 emission slightly decreases while both NPV and MP increases.

Multiobjective optimization formulation

To find different states of optimal operation, a set of single-objective optimization problems applying the ε-constraint method[4] was solved using MINLP solvers in GAMS to find the optimal NPV s corresponding to given amounts of specific emissions at constant CO_2 emission and sequestration costs (52 $/$t_{CO2}$ and 26 $/$t_{CO2}$). An advantage of a multiobjective approach is that it provides solutions from which one may select a suitable compromise based on both economic and environmental aspects. Because the objectives are nondominated, they can be represented as a Pareto Frontier in a diagram, compare Figure 9.

Table 5. Results from the Model for Four Selected Point in the Frontier Diagram (Figure 9).

	1	2	3	4
NPV (G$)	0.49	1.28	1.89	2.05
Specific emission (t_{CO2}/t_{ls})	0.45	0.55	0.75	0.98
Coal flow rate (t/h)	0.0	0.0	80.1	80.2
Ore flow rate (t/h)	133.1	133.1	153.6	153.6
External coke rate (t/h)	56.1	52.6	0.0	0.0
Limestone rate (t/h)	25.1	24.8	23.5	23.5
Quartzite rate (t/h)	0.0	0.0	0.0	0.0
Pellet rate (t/h)	90.0	90.0	70.2	70.2
Air volume rate (knm^3/h)	106.5	113.0	113.0	113.0
Oxygen flow rate (knm^3/h)	22.0	17.3	17.8	18.7
Slag rate (kg/t_{hm})	220	218.4	216.2	216.2
Scrap rate (t/h)	37.5	37.5	37.5	37.5
Nitrogen flow rate (t/h)	47.2	56.0	56.0	56.0
DME flow rate (t/h)	0.0	0.0	0.0	0.6
Oil flow rate (t/h)	21.64	21.9	18.0	18.0
CO_2 sequestrated (t/h)	148.7	118.8	116.1	81.6
Methanol production (t/h)	23.4	20.9	21.2	19.3
Steel cost ($/$t$ls)	358.4	355.1	300.3	311.0

Data are estimated by using MINLP solvers in GAMS and maximum NPV is reported.

The results show that for lower emission states CDR and LP methanol reactor and for higher NPV s POR and GP methanol reactor are dominant unit processes. In all states, TSA is selected for carbon monoxide recovery, PSA for hydrogen recovery, and amine-based chemical absorption for carbon dioxide capturing. Table 5 shows some of the variables (main inputs and outputs from the system) extracted from the model for the four points (1–4) indicated in Figure 9. Due to relaxed constraints on external district heat and electricity in the power plant and the price of them, no external district heat and electricity is produced. In the low emission scenario (cf. point 1), a supply of external coke, even though it is more expensive, is needed (for "outsourcing the emissions"), resulting in increase in the production costs of steel. To reach the minimum emission from the integrated

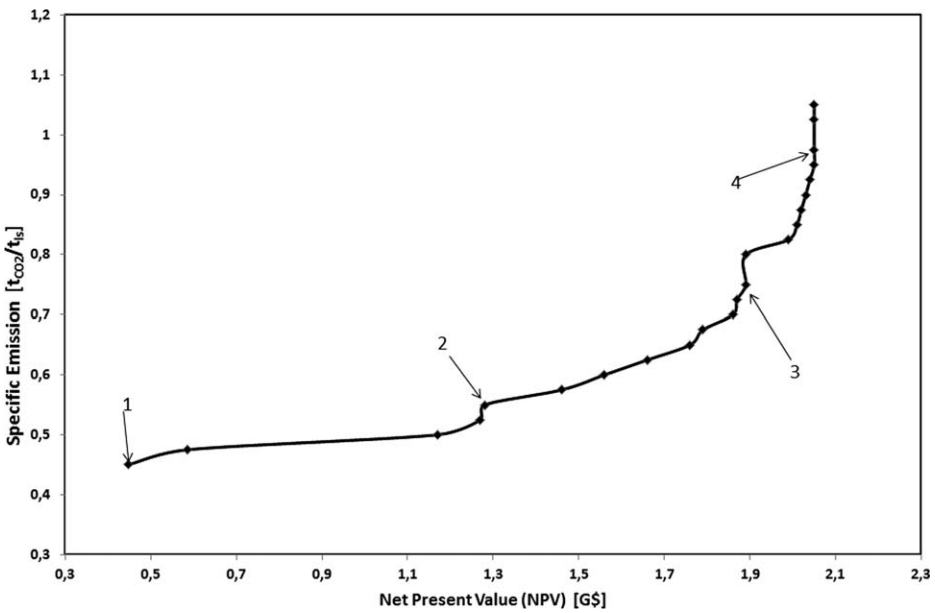

Figure 9. Pareto frontier for maximization of net present value and minimization of specific emission rate for a steel plant integrated with a polygeneration system, at a hot metal production rate of 150 t_{hm}/h and constant costs of emission and sequestration (52 $/$t_{CO2}$ and 26 $/$t_{CO2}$).

Points 1–4 indicated by arrows refer to the optimal states reported in detail in Table 5.

steelmaking plant studied, an increase of more than 50 $\$/t_{ls}$ would be expected in the costs of steel production.

Conclusions and Future Work

In this article, a superstructure for an integrated steelmaking plant combined with a polygeneration system has been proposed to find optimal operation and design states with respect to process economics for different scenarios of carbon dioxide emission and sequestration costs. Generalized disjunctive programming was used to model the system and to investigate both profitability and environmental impacts while optimizing the mass and energy flows in the system according to different technologies. The results show that by applying a process integration approach it is possible to suppress half of the emissions from a conventional steelmaking plant. Depending on the importance given to low costs or low emission rates, the solutions of a multiobjective formulation illustrated that different design concepts were applied in different regions.

Future work will be focused on an analysis of using alternative fuels, such as natural gas and biomass, in the system, also considering different BF technologies, such as top gas recycling and cold oxygen injection. The study could also be extended to steelmaking plants with multiple BFs, and should also consider the end units of the steelmaking process, that is, continuous casting and rolling. It would also be possible to study the system with a focus on different product demands to gain insight into how steelmaking could be developed in a more sustainable direction.

Acknowledgments

Financial support from the Academy of Finland within the SYMBIOSIS project and from the Fortum foundation, Finland, are gratefully acknowledged. H.G. would also like to thank the CAPD members and visitors in Carnegie Mellon University for their support.

Literature Cited

1. Liu P, Pistikopoulos EN, Li Z. A mixed-integer optimization approach for polygeneration energy systems design RID C-4913-2011 RID E-7840-2011. *Comput Chem Eng*. 2009;33:759–768.
2. Zhang Y, Ni W, Li Z. Research on superclean polygeneration energy system of iron and steel industry. In: Power and Energy Systems, Proceeding of the 7th IASTED International Conference on Power and Energy Systems. *Anaheim: Acta Press*, 2004:152–157.
3. Liu P, Gerogiorgis DI, Pistikopoulos EN. Modeling and optimization of polygeneration energy systems RID C-4913-2011. *Catal Toda y*. 2007;127:347–359.
4. Liu P, Pistikopoulos EN, Li Z. A Multiobjective optimization approach to polygeneration energy systems design RID C-4913-2011 RID E-7840-2011. *AIChE J*. 2010;56:1218–1234.
5. Chen Y, Adams TA II, Barton PI. Optimal design and operation of flexible energy polygeneration systems. *Ind Eng Chem Res*. 2011;50:4553–4566.
6. Chen Y, Adams TA II, Barton PI. Optimal Design and Operation of Static Energy Polygeneration Systems. *Ind Eng Chem Res*. 2011;50:5099–5113.
7. Ghanbari H, Helle M, Pettersson F, Saxen H. Optimization study of steelmaking under novel BF operation combined with methanol production. *Ind Eng Chem Res*. 2011;50:12103–12112.
8. Ghanbari H, Helle M, Saxén H. Process integration of steelmaking and methanol production for suppressing CO2 emissions—a study of different auxiliary fuels. *Chem Eng Process*. 2012;61:58–68.
9. Helle H, Helle M, Saxen H. Nonlinear optimization of steel production using traditional and novel blast furnace operation strategies. *Chem Eng Sci*. 2011;66:6470–6481.
10. "PLS_Toolbox 6.5.2" Advanced Chemometrics software for use with Matlab, Eigenvector research incorporated, 2011. Accessible at: http://www.eigenvector.com/software/pls_toolbox.htm
11. Lophaven SN, Nielsen HB, Sondergaard J. Aspects of the Matlab toolbox DACE, IMM-REP-2002-13, 2002; Accessible at: http://www2.imm.dtu.dk/~hbni/dace/
12. Costello R. COPure^{SM} Process; R.C. Costello & Assoc, Inc., Private communication, 2011.
13. Rabo JA, Francis JN, Angell CL. Selective adsoption of carbon monoxide from gas streams, Patent US4019879 A, 1977.
14. Olajire AA. CO2 capture and separation technologies for end-of-pipe applications—a review. *Energy*. 2010;35:2610–2628.
15. Tobiesen FA, Svendsen HF, Mejdell T. Modeling of blast furnace CO2 capture using amine absorbents. *Ind Eng Chem Res*. 2007;46:7811–7819.
16. Lie JA, Vassbotn T, Hägg M, Grainger D, Kim T, Mejdell T. Optimization of a membrane process for CO2 capture in the steelmaking industry. *Int J Greenh Gas Control*. 2007;1:309–317.
17. Ruthven DM, Farooq S, Knaebel KS. Pressure Swing Adsorption. VCH Wiley, October 1, 1993, ISBN-10: 0471188182, ISBN-13: 978-0471188186.
18. Porter MC. The separation of gases by membrane. In: Handbook of Industrial Membrane Technology, William Andrew Publishing/Noyes, 1990:559. ISBN:978-0-8155-1205-9.
19. Henis JMS, Tripodi MK. Multicomponent Membrane for Gas Separations, Patent US4230463 A, 1980.
20. Van Dijk CP, Solbakken A, Rovner JM. Methanol from Coal and Natural Gas, Patent US4407973, 1983.
21. Wang S, Lu G, Millar G. Carbon dioxide reforming of methane to produce synthesis gas over metal-supported catalysts: state of the art RID C-5507-2008 RID A-2859-2008. *Energy Fuels*. 1996;10:896–904.
22. Zhu J, Zhang D, King K. Reforming of CH4 by partial oxidation: thermodynamic and kinetic analyses. *Fuel*. 2001;80:899–905.
23. Biegler LT, Grossmann IE, Westerberg AW. Systematic Methods of Chemical Process Design. Upper Saddle River, NJ: Prentice Hall PTR, 1997.
24. Vaswani S. Development of Models for Calculating the Life Cycle Inventory of Methanol by Liquid Phase and Conventional Production Process. Department of Civil Engineering: Raleigh, NC, 2000.
25. The National Institute of Standards and Technology. NIST Chemistry Webbook, 2011. Available online at http://webbook.nist.gov/chemistry/.
26. GAMS Development Corporation, 2011. GAMS (General Algebraic Modeling System) Software v23.7.3. Available at: http://www.gams.com.
27. Tawarmalani M, Sahinidis N. A polyhedral branch-and-cut approach to global optimization. *Math Program*. 2005;103:225–249.
28. Duran M, Grossmann I. An outer-approximation algorithm for a class of mixed-integer nonlinear programs. *Math Program*. 1986;36:307–339.

Manuscript received Jul. 19, 2012, revision received Dec. 7, 2012, and final revision received Mar. 16, 2013.